Testing Program

In addition to visual inspections, a program of field and laboratory testing was conducted to evaluate the in-place properties of the concrete in the Bonner Bridge. Field testing included taking concrete core samples, half cell potential corrosion measurements, and ultrasonic pulse velocity measurements. Laboratory testing included compressive strength tests, petrographic studies, and determination of chloride ion concentrations in the concrete.

Field Testing Methodology

Field work for this assessment was performed from March through April 2006. During this field investigation period, the following tasks were performed on selected high bent structures:

- Half-cell potential corrosion measurements (HCP) were made on selected elements including the pile caps, vertical surfaces of the bent frames, the bent caps, the vertical surfaces of the girders, and the top surface of the bridge deck. The purpose of the HCP testing was to assess the potential for corrosion of the mild reinforcement.
- Ultrasonic pulse velocity measurements were made on selected elements including the pile caps, vertical surfaces of the bent frames, the bent caps and the vertical surfaces of the girders. The ultrasonic pulse velocity measurements were made to assess the integrity of the concrete. Figures 7, 8, 9, and 10 illustrate the location of the UPV and half-cell measurements on the high bents and approach bents, respectively.
- Core sampling was completed to collect a series of concrete samples from selected bents, prestressed girders, and bridge deck slabs for testing and evaluation in the laboratory. Four inch diameter cores were removed from the bent structures and 3 1/2" diameter cores were removed from the bridge deck and elsewhere if the laboratory tests did not include compressive strength testing.

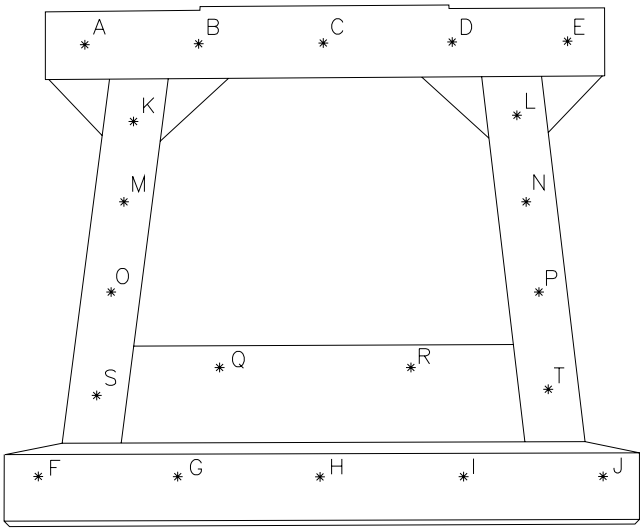

Figure 7. Typical UPV and Half Cell testing locations on the single frame bents.

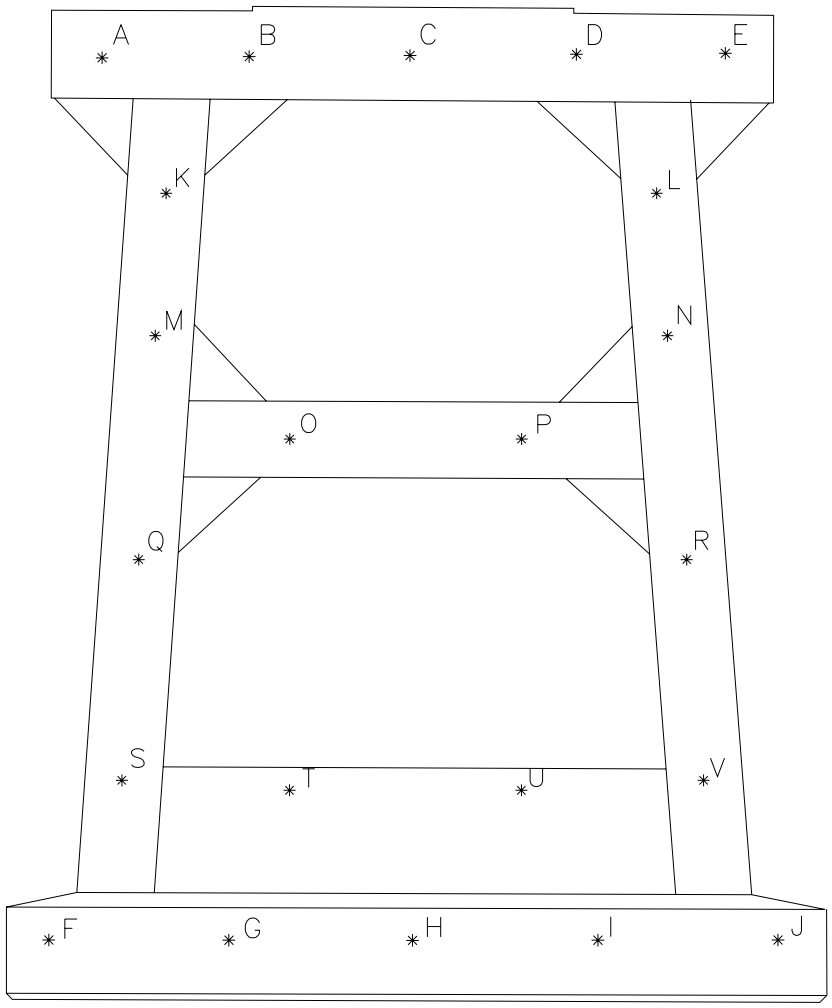

Figure 8. Typical UPV and Half Cell testing locations on the two frame bents.

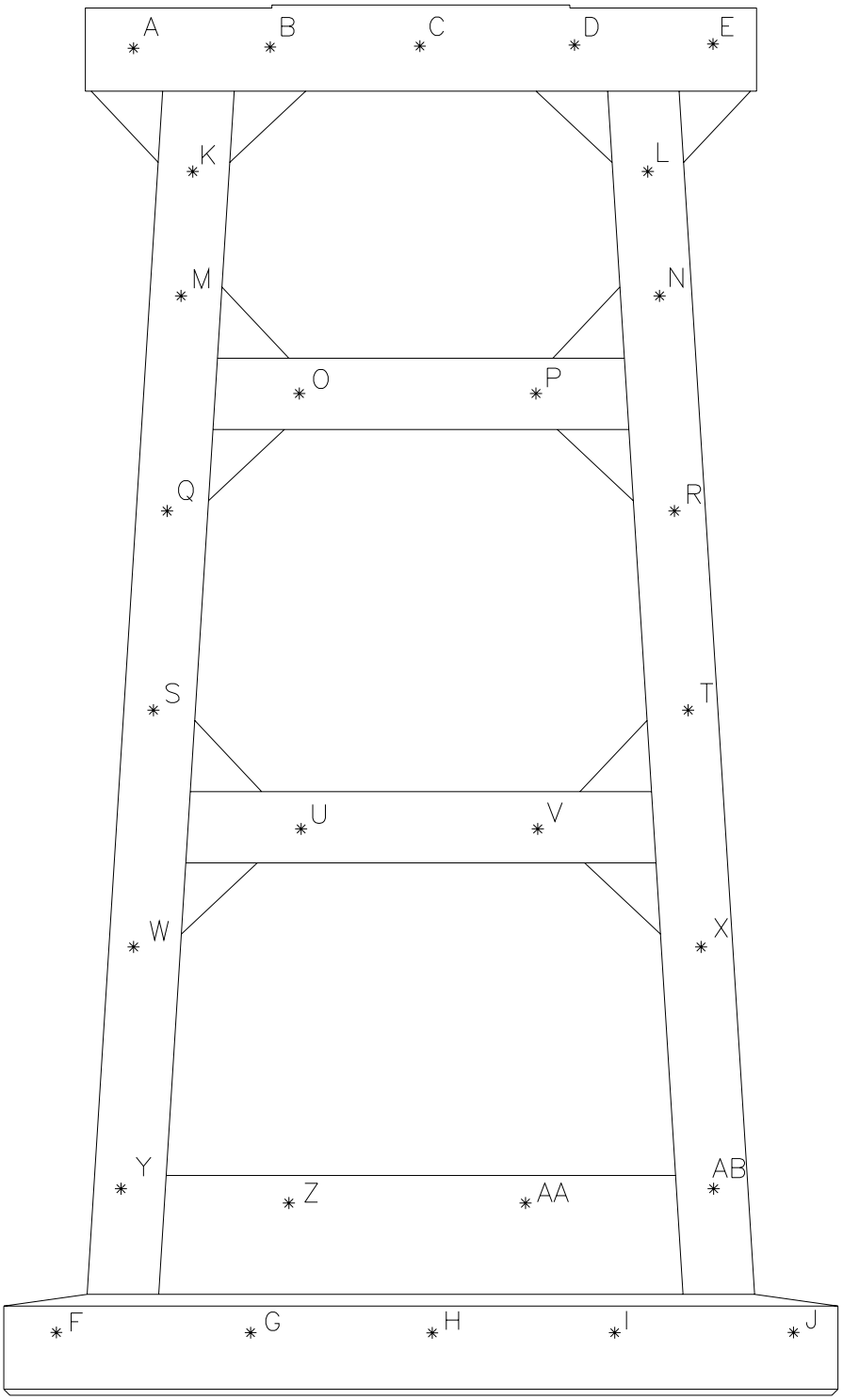

Figure 9. Typical UPV and Half Cell testing locations on the three frame bents.

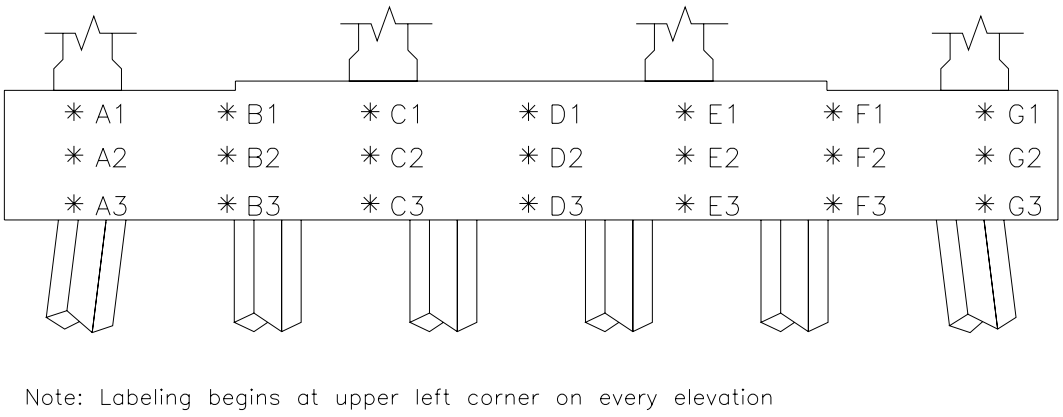

Figure 10. Typical UPV and Half Cell testing locations on the pile bents.

Field Testing Findings

Coring

A series of core samples were removed from selected bents, prestressed girders and bridge deck slabs. Four inch diameter cores were removed from the bent structures and 3 1/2" diameter cores were removed from the bridge deck and other locations where the laboratory tests did not include compressive strength and ultrasonic pulse velocity testing. Detailed field inspection sheets were used to identify the coring locations so that cores were taken from areas and elements that appeared to be in moderate, poor and severely deteriorated conditions. Several of the cores were taken through reinforcing bars to extract them for visual examination of their corrosion condition. A summary of all cores tested is included in Table 9.

Half- Cell Corrosion Measurements

Half-cell potentials (HCP or corrosion potentials) were measured according to ASTM C 876, *Standard Test Methods for Half-Cell Potentials of Uncoated Reinforcing Steel in Concrete*, to investigate the thermodynamic corrosion tendency of the reinforcing bars. Corrosion potentials do not indicate how fast corrosion is taking place but rather measure the amount of iron dissolved in the concrete pore solution and so give an indication of the corrosion risk. According to ASTM C876, the three ranges of measured potentials and the corresponding indicators of corrosion are as follows:

A. More positive than -200mV: Greater than 90% probability that no steel corrosion is occurring at the time of testing.

B. More negative than -350mV: Greater than 90% probability that steel corrosion is occurring at the time of testing.

C. Between -200mV and -350mV: Corrosion activity is uncertain.

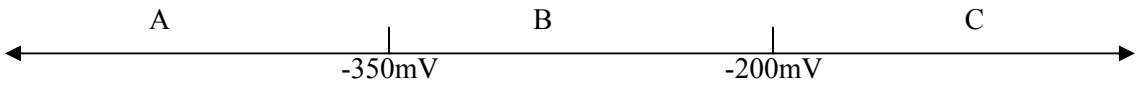

Although the above corrosion indicators are widely accepted as a means of determining the likelihood of steel corrosion, the range values become less important in situations where carbonation of the concrete

cover has occurred. Instead, the relative difference between measured potentials within concrete members or structures becomes the important factor.

A high internal impedance, digital multimeter was employed for the testing by connecting the positive terminal to a reinforcing bar and the negative terminal to a copper-copper sulfate reference electrode (CSE). By doing this, the corrosion potential of the bar could be measured with respect to the CSE, which had a known potential.

When performing the HCP measurements an electrical connection (grounding) was made to the reinforcement and potentials were measured using a digital voltmeter with a 100 M-ohm internal impedance by placing a CSE at the intersections of a grid. A HCP contour map was generated for each test area based on the data collected.

Before commencing HCP measurements an electrical continuity test was performed at each site to verify the degree of electrical continuity between two distant electrical connections to the reinforcing steel within the element. Electrical continuity is a critical component for a valid HCP measurement because if there is relatively high resistance between the two grounding points, HCP measurements will be influenced by the resistance. Half-cell potential measurements were made at the twelve bents selected for up-close inspection. In addition, half cell testing was performed on the top surface of the bridge deck in 13 of the high level spans. Finally, localized HCP measurements were taken on the sides of girders in six of the high level spans.

The HCP measurements were taken on the bent as shown on the detailed inspection sheets in Appendix D.1A-D.1D. The locations for the HCP measurements on the bents are shown in Figures 7, 8, 9, and 10. For the HCP's taken on the bridge deck, measurements were taken at three locations across half the roadway width and spaced approximately 5' along the length of the span. The HCP measurements on the girders were taken on a 6" by 6" grid over an area approximately 60" long and the full depth of the girder. HCP data is summarized in Tables 4a, 4b, and 5 for the single frame bents, triple frame bents, and approach spans respectively. HCP measurements taken on both the girders and bridge decks are shown as contour plots in Appendix D.3.

Table 4a. Half-cell potential measurements for the inspected high level bents

Half-Cell Potential Readings for Single Frame Bents (units = volts)													
	Bent:	129		160		161		163		164			
	Elevation:	North	South	North	South	North	South	North	South	North	South		
Bent Cap	A		-0.152		-0.294	-0.214		-0.251		-0.355		A	Bent Cap
	B		-0.354									B	
	C				-0.350	-0.249		-0.349		-0.372		C	
	D		-0.218									D	
	E		-0.153		-0.284	-0.309		-0.373		-0.457		E	
Frame	K				-0.134	-0.268		-0.241		-0.358		K	Frame
	L				-0.197	-0.325		-0.367		-0.343		L	
	M				-0.121	-0.125		-0.369		-0.418		M	
	N				-0.283	-0.476		-0.245		-0.385		N	
	O				-0.258	-0.379		-0.358		-0.452		O	
	P				-0.289	-0.433		-0.265		-0.438		P	
	Q		-0.332		-0.460	-0.313		-0.231		-0.286		Q	
	R		-0.160		-0.226	-0.393		-0.188		-0.311		R	
	S				-0.275	-0.544		-0.335		-0.514		S	
	T		-0.323		-0.368	-0.433		-0.306		-0.409		T	
Pile Cap	F			-0.498	-0.359			-0.428	-0.366	-0.286	-0.389	F	Pile Cap
	G	-0.332	-0.286									G	
	H	-0.302	-0.160			-0.451		-0.479	-0.438		-0.398	H	
	I	-0.260	-0.395							-0.320		I	
	J			-0.372	-0.306	-0.363		-0.418	-0.317		-0.412	J	

Table 4b. Half-cell potential measurements for the inspected high level bents

Half-Cell Potential Readings for Triple Frame Bents (units = volts)											
	Bent:	140		145		149		150			
	Elevation:	North	South	North	South	North	South	North	South		
Bent Cap	A		-0.166		-0.321		-0.326			A	Bent Cap
	B		-0.462		-0.399				-0.255	B	
	C				-0.130		-0.336		-0.353	C	
	D		-0.450		-0.219		-0.283			D	
	E		-0.360		-0.228				-0.311	E	
Top Frame	K									K	Top Frame
	L									L	
	M		-0.172		-0.233					M	
	N		-0.180		-0.241					N	
	O		-0.136		-0.189		-0.380		-0.438	O	
	P				-0.175		-0.241		-0.155	P	
Middle Frame	Q				-0.405					Q	Middle Frame
	R								-0.140	R	
	S		-0.362							S	
	T									T	
	U		-0.157		-0.256		-0.287			U	
	V		-0.266		-0.255					V	
Bottom Frame	W						-0.329			W	Bottom Frame
	X		-0.467				-0.476			X	
	Y		-0.187	-0.360		-0.390		-0.518		Y	
	Z		-0.305		-0.202	-0.309		-0.224		Z	
	AA		-0.342		-0.409	-0.271		-0.259		AA	
	AB		-0.245	-0.297		-0.462		-0.420		AB	
Pile Cap	F	-0.449		-0.235	-0.318	-0.495	-0.395	-0.419	-0.522	F	Pile Cap
	G		-0.493							G	
	H	-0.467	-0.344	-0.245	-0.216	-0.282	-0.585	-0.380	-0.421	H	
	I									I	
	J	-0.473	-0.418	-0.519	-0.235	-0.406	-0.513	-0.544	-0.423	J	

Table 5. Half-cell potential measurements for the inspected approach bents

Half-Cell Potential Readings for Approach Bents (units = volts)									
Bent #	**Elevation**	**Position**	**A**	**B**	**C**	**D**	**E**	**F**	**G**
7	**South**			-0.050		-0.263			-0.120
12	**North**		-0.300	-0.372	-0.210		-0.120		
	South			-0.137			-0.347		-0.314
13	**South**		-0.047			-0.200			-0.105
21	**North**	1	-0.084	-0.430		-0.417		-0.165	-0.109
		2	-0.288	-0.433		-0.425		-0.202	-0.176
		3	-0.169	-0.385		-0.438		-0.206	-0.140
	South	1	-0.154	-0.234		-0.396		-0.239	-0.136
		2	-0.250	-0.195		-0.391		-0.262	-0.129
		3	-0.365	-0.169		-0.358		-0.276	-0.142
31	**North**	1	0.176	-0.217		-0.275		-0.276	-0.143
		2	-0.254	-0.208		-0.316		-0.297	-0.166
		3	-0.164	-0.147		-0.170		-0.143	-0.159
	South	1	-0.247	-0.242		-0.298			-0.193
		2	-0.280	-0.276		-0.319			-0.229
		3	-0.717	-0.318		-0.266			-0.087
53	**North**	1	-0.191	-0.257		-0.233		-0.213	-0.227
		2	-0.162	-0.187		-0.265		-0.244	-0.190
		3	-0.120	-0.123		-0.160		-0.188	-0.123
	South	1	-0.136	-0.372		-0.323		-0.353	-0.195
		2	-0.197	-0.298		-0.223		-0.256	-0.099
		3	-0.163	-0.202		-0.206		-0.218	-0.099
75	**South**		-0.199		-0.300		-0.285		-0.262
88	**South**		-0.081		-0.273		-0.290		-0.216
93	**South**		-0.389			-0.377			-0.340
102	**South**		-0.244				-0.262		-0.305
103	**South**		-0.149			-0.294			-0.236
116	**South**		-0.302			-0.299		-0.247	
117	**South**			-0.131		-0.233		-0.371	
175	**South**			-0.387		-0.315		-0.377	
176	**South**			-0.369		-0.320		-0.393	
177	**South**			-0.313		-0.350		-0.426	-0.443
178	**North**					-0.397		-0.463	
187	**North**		-0.317	-0.304		-0.334			-0.245
190	**North**		-0.220			-0.327		-0.210	
193	**North**		-0.142	-0.218		-0.272		-0.239	
201	**North**		-0.162		-0.301		-0.234		

Ultrasonic Pulse Velocity Testing

Ultrasonic pulse velocity (UPV) testing was conducted in the field to assess the condition of pile caps, bent columns, bent caps, and girders. This testing provides two indicators of overall conditions in the concrete components. First is an indication of the overall quality of the concrete in one location compared to other locations. This test compares velocity measurements with measurements collected on concrete core samples tested in the laboratory. The second indication from the ultrasonic pulse velocity data is the identification of underlying discontinuities in the concrete elements.

UPV measurements are summarized in Tables 6a, 6b, & 6c for inspected high level bents and Table 7 for inspected approach bents. UPV data for both the high level bents and approach bents was recorded on detailed inspection sheets that can be found in Appendix D. UPV measurements were made at the locations noted in Figures 7, 8, 9, and 10.

In general, UPV measurements made in concrete areas that appeared sound indicated concrete of good quality and absent of voids or discontinuities. In these areas, UPV measurements typically ranged from 11,500 to 14,000 fps. UPV measurements taken in zones where patches or delaminations were observed typically ranged from 6,500 to 9,000 fps.

Tables 6a. UPV measurements for the inspected high level bents

UPV Readings for Single Frame Bents (units = ft/s)													
	Bent:	129		160		161		163		164			
	Elevation:	North	South	North	South	North	South	North	South	North	South		
Bent Cap	A		14,200 V		13,900							A	Bent Cap
	B					13,300		14,000			14,400	B	
	C		12,500 V		12,800	13,800		14,200			13,600	C	
	D					13,500		13,700			13,500	D	
	E		7,200 V		13,300							E	
Frame	K					7,900					7,100	K	Frame
	L					6,300		14,000			8,900	L	
	M				14,200			12,000				M	
	N				14,700			14,200				N	
	O		14,500		7,500	9,100		15,000			14,600	O	
	P		14,100		14,300			12,000			13,800	P	
	Q		14,600	14,400		14,000			14,200	13,600		Q	
	R		13,800	14,900		13,800			14,600	14,200		R	
	S							.			7,100	S	
	T					4,600					13,100	T	
Pile Cap	F	9,400 V	5,300		6,000	5,400			5,200		6,000	F	Pile Cap
	G											G	
	H				6,100	7,400			5,800			H	
	I	14,200 V	14,400									I	
	J	14000 V	10,500		5,500	5,500			6,700		6,000	J	
"V" denotes a reading taken vertically.													

Tables 6b. UPV measurements for the inspected high level bents

UPV Readings for Double Frame Bents (units = ft/s)									
	Bent:	135		153		154			
	Elevation:	North	South	North	South	North	South		
Bent Cap	A						14,000	A	Bent Cap
	B		10,700 V	12,900				B	
	C			13,400			13,100	C	
	D		15,400 V					D	
	E						14,100	E	
Top Frame	K							K	Top Frame
	L							L	
	M			14,400		12,000		M	
	N			14,100		7,300		N	
	O		7,400 V	13,900 V		13,700		O	
	P							P	
Bottom Frame	Q							Q	Bottom Frame
	R		8,800					R	
	S		3,800				12,900	S	
	T		13,400	13,000			11,100	T	
	U		14,700	12,300			13,000	U	
	V		14,900	14,500			11,200	V	
Pile Cap	F		12,800				6,800	F	Pile Cap
	G			4,600				G	
	H		12,900	13,300			3,600 *	H	
	I							I	
	J		13,900	7,000			3,600 *	J	

"V" denotes a reading taken vertically.

* Denotes Unsteady Signal

Tables 6c. UPV measurements for the inspected high level bents

UPV Readings for Triple Frame Bents (units = ft/s)											
	Bent:	140		145		149		150			
	Elevation:	North	South	North	South	North	South	North	South		
Bent Cap	A				12,000					A	Bent Cap
	B		12,500 V				14,200 V		14,400 V	B	
	C				13,600		13,800 V		13,600 V	C	
	D		11,300 V				13,700		13,600	D	
	E				14,200					E	
Top Frame	K									K	Top Frame
	L									L	
	M								6,500	M	
	N				14,400				14,200	N	
	O				13,700		13,000 V		6,500 V	O	
	P		13,300		13,900					P	
Middle Frame	Q				9,700					Q	Middle Frame
	R		14,200				13,800			R	
	S		13,300				12,600			S	
	T				11,800					T	
	U		11,800 V		14,000		14,000 V			U	
	V		13,100							V	
Bottom Frame	W									W	Bottom Frame
	X		13,100				14,300			X	
	Y		13,700		14,100		14,000		11,200	Y	
	Z		13,500		14,000		14,300		10,700	Z	
	AA		14,300		14,700		14,300		13,600	AA	
	AB		13,800		14,400		13,400		13,600	AB	
Pile Cap	F	6,400				13,900				F	Pile Cap
	G	13,000								G	
	H					6,600			13,700	H	
	I					6,600			13,700	I	
	J	7,300								J	

"V" denotes a reading taken vertically.

Table 7. UPV measurements for the inspected approach bents

UPV Readings for Approach Bents (units = ft/s)								
Bent #	**Elevation**	**A**	**B**	**C**	**D**	**E**	**F**	**G**
7	**South**		13,800			13,800		14,100
12	**North**	12,400	13,100	12,800		13,400		12,900
	South		12,900	7,300 V	13,200	13,000		12,100
13	**North**		12,700		12,300		13,200	12,700
75	**South**		13,500 V		13,900 V			13,400
88	**South**		12,700	13,100	12,900			13,200
93	**South**	14,100 V	13,800		13,700	14,000 V	13,500	13,700 V
102	**South**		12,700		13,400			13,700
103	**South**	13,600 V				13,500 V		13,300 V
116	**South**		12,000		10,700		12,900	
117	**South**	13,000	13,200		13,200			
175	**South**	10,400			9,200			11,900
176	**North**		13,200		13,100		12,800	
177	**South**		13,000		11,200		12,300	
178	**North**		12,700		12,800		11,200	
187	**North**	13,100			13,300		12,900	
190	**South**	10,600			8,600	12,200		5,700
193	**South**		12,500			6,900	10,900	
						12,400	12,000	
							13,300	
201	**South**	13,900		13,600				13,500

"V" denotes a reading taken vertically.

Laboratory Testing

In the laboratory, the cores were analyzed to determine compressive strength, the chloride ion concentration, carbonation depth, condition and chemistry of the steel, and the concrete quality.

Compressive Strength Tests

A series of cores were removed from the bridge and tested in compression according to ASTM C39, *Standard Test Method for Compressive Strength of Cylindrical Concrete Specimens* and ASTM C42, *Standard Test Method for Obtaining and Testing Drilled Cores and Sawed Beams of Concrete*. The ends of the cores that were received were cut parallel and, where possible, a core length-to-diameter (L/D) ratio of two was tested. The cores were tested in the as-received condition.

When a core length-to-diameter ratio of two was not possible, correction factors as given by ASTM C42, *Standard Test Method for Obtaining and Testing Drilled Cores and Sawed Beams of Concrete*, were applied. The correction is necessary since the strength measured in cores with L/D lower than two will be artificially high due to the effects of end restraint during testing. However, these correction factors in this standard apply explicitly only up to strengths of 6,000 psi. According to the standard method, the correction factor, "should be applied to high strength concrete with caution." When the correction factors were used with strengths over 6,000 psi, it was noted in the report.

A summary of compressive strength tests conducted on cores from the bridge is shown in Table 8. A summary of all physical testing on cores removed from the bridge is shown in Table 10 at the end of the

Testing Program section. The average compressive strength for various parts of the bridge were as follows:

- The compressive strength of the cores tested ranged from 3,830 - 8,550 psi with all but three of the 51 cores testing above 5,000 psi.
- The average compressive strength for all 51 cores tested was 6,497 psi.
- The average compressive strength for all cores from the bents was 6,482 psi.
- The average compressive strength for all cores from the prestressed concrete girders was 7,170 psi.
- The average compressive strength for all cores from the bridge deck was 5,928 psi.

These compressive strengths are representative of high quality concrete.

Table 8. Summary of compressive strength tests

Core No.	Location Description	Length (in.)	Diameter (in.)	L/D Correction	Compressive Strength (psi)	Corrected Compressive Strength (psi)
High Level Spans						
16	Bent 129 - Pile Cap	7.600	3.733	2.04	6,320	--
21	Bent 135 - Pile Cap	7.680	3.733	2.06	5,340	5,340
29	Bent 145 - Pile Cap	7.741	3.728	2.08	3,830	
33	Bent 149 - Pile Cap	7.650	3.732	2.05	5,720	5,720
41	Bent 150 - Pile Cap	7.741	3.727	2.08	6,680	
55	Bent 161 - Pile Cap	7.612	3.730	2.04	7,870	--
58	Bent 163 - Pile Cap	7.680	3.734	2.06	5,790	5,790
15	Bent 129 - Column	7.652	3.735	2.05	6,580	
20	Bent 135 - Column	5.811	3.728	1.56	7,740	
30	Bent 145 -Column	4.860	3.728	1.30	7,440	
31	Bent 145 - Column	7.219	3.726	1.94	6,480	
32	Bent 149 - Column	7.564	3.728	2.03	6,870	--
34	Bent 149 - Column	7.607	3.736	2.04	6,450	--
37	Bent 150 - Column	5.471	3.707	1.48	7,650	
39	Bent 150 - Column	6.505	3.724	1.75	5,780	5,660
40	Bent 150 - Column	4.627	3.728	1.24	5,610	5,200
53	Bent 161 - Column	7.711	3.734	2.07	7,190	--
57	Bent 163 - Column	5.837	3.469	1.68	8,430	
14	Bent 129 - Bent Cap	7.538	3.729	2.02	4,420	4,420
18	Bent 135 - Bent Cap	7.395	3.722	1.99	5,490	5,490
28	Bent 145 - Bent Cap	7.333	3.732	1.96	7,530	
54	Bent 161 - Bent Cap	7.540	3.726	2.02	6,840	
56	Bent 163 - Bent Cap	7.730	3.730	2.07	7,640	--
13	Span 129 - Girder	7.322	3.733	1.96	8,310	
113	Span 149 - Girder	6.641	3.265	2.03	6,720	
91	Span 130 - Deck	5.980	3.249	1.84	5,360	5,360

92	Span 132 - Deck	5.695	3.246	1.75	5,310	5,200
115	Span 150- Deck	3.638	3.246	1.12	7,470	
136	Span 162 - Deck	4.902	3.245	1.51	5,570	5,350
Approach Spans						
Core No.	Location Description	Length (in.)	Diameter (in.)	L/D Correction	Compressive Strength (psi)	Corrected Compressive Strength (psi)
1	Bent 7 - Pile Cap	7.425	3.725	1.99	6,920	--
2	Bent 12 - Pile Cap	7.513	3.721	2.02	4,990	4,990
3	Bent 13 - Pile Cap	7.445	3.725	2.00	5,930	5,930
4	Bent 88 - Pile Cap	7.472	3.732	2.00	6,250	--
6	Bent 93 - Pile Cap	6.043	3.738	1.62	8,550	--
8	Bent 102 - Pile Cap	7.391	3.735	1.98	5,600	5,600
9	Bent 102 - Pile Cap	7.490	3.736	2.01	6,150	--
10	Bent 116 - Pile Cap	7.472	3.725	2.01	6,290	--
12	Bent 117 - Pile Cap	7.425	3.732	1.99	5,730	5,730
63	Bent 167 - Pile Cap	7.431	3.730	1.99	6,400	--
64	Bent 175 - Pile Cap	4.800	3.728	1.29	6,830	--
65	Bent 176 - Pile Cap	6.076	3.734	1.63	7,180	--
66	Bent 177 - Pile Cap	4.890	3.722	1.31	7,240	--
67	Bent 178 - Pile Cap	3.430	3.716	1.00	8,200	--
68	Bent 187 - Pile Cap	6.127	3.725	1.64	6,310	--
69	Bent 190 - Pile Cap	7.412	3.716	1.99	5,930	5,930
70	Bent 193 - Pile Cap	7.405	3.716	1.99	5,890	5,890
71	Bent 201 - Pile Cap	7.474	3.724	2.01	6,080	--
5	Span 93 - Girder	7.072	3.729	1.90	7,450	--
147	Span 176 - Girder	6.705	3.243	2.07	6,200	--

Ultrasonic Pulse Velocity Measurements on Cores

At the time each concrete core sample was prepared for compressive strength testing, ultrasonic pulse velocity measurements were made. These measurements were made after the cores were trimmed to length but before the core samples were capped for compressive strength testing.

The relationship between UPV measurements and concrete compressive strength data for these cores is shown in the graph in Figure 11. Because the overall concrete compressive strengths are generally between 5,000 and 8,000 psi and the

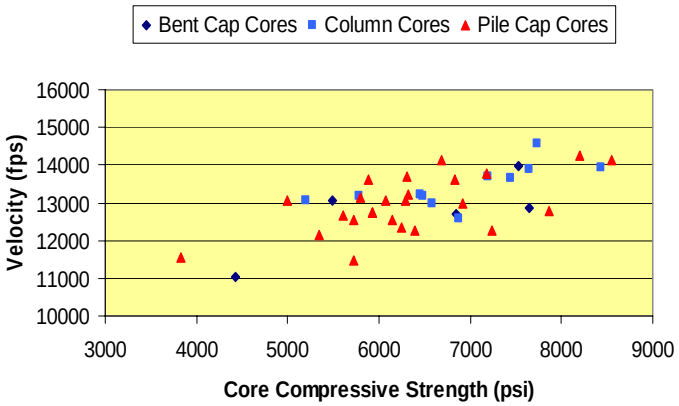

Figure 11. Comparison of Compressive Strength to UPV

concrete appears to be of high quality (good consolidation and well blended), the resulting ultrasonic pulse velocities are in a fairly narrow range extending from 12,000 to 14,500 fps which are velocities generally associated with good quality concrete. More significant is the narrow band of velocities which indicates uniformity in the concrete from one location to another.

Petrographic Examination

A series of cores were selected for petrographic examination in order to characterize the quality of concrete. Carbonation was also tested by breaking the cores and applying phenolphthalein solution onto freshly exposed concrete surfaces. Carbonation is the reaction of carbon dioxide in the atmosphere with hydroxides in the concrete. This reaction neutralizes the cement and ultimately lowers the pH of the concrete, which can depassivate the steel and contribute to corrosion.

The cores were chosen to include representative samples of the concrete from girders, pile caps, and the deck. Detailed petrographic studies were conducted on Core 17 (Span 132, Girder 4), Core 120 (Bent 150 Pile Cap), and Core 114 (Span 150, Mid-span Deck). Brief petrographic studies were conducted on Core 138 (Span 162, Girder 3), Core 103 (Bent 145 Pile Cap), Core 90 (Span 130, Mid-span Deck), Core 93 (Span 132, Mid-span Deck), Core 137 (Span 162, Mid-span Deck), Core 104 (Bent 145 Middle Column), and Core 117 (150 Middle Column).

Methods

The petrographic studies were performed in general accordance with the procedures outlined in ASTM C 856, *Standard Practice for Petrographic Examination of Hardened Concrete*. The samples were examined visually, photographed, and measured. A longitudinal slice was cut from each of the cores, and one side was lapped for detailed study. The lapped sections were examined at magnifications ranging from approximately 5X to 50X using a stereomicroscope. Powder immersion mounts were prepared from representative locations. These preparations were studied using a polarized-light (petrographic) microscope to evaluate the mineralogy and microstructure of the concrete and aggregates. Portions of each sample were fractured in the laboratory using a geology hammer, and the fresh fracture surfaces were studied using a stereomicroscope. Qualitative tests and various staining procedures were employed as needed to study carbonation and absorption characteristics.

Girders

Core 17 - Span 132, Girder 4

The concrete contained well graded siliceous coarse and fine aggregates uniformly dispersed in a non-air-entrained, light gray, Portland cement paste. The estimated air content was 2 to 4 percent. The concrete was well consolidated, but contained a few large entrapped air voids. The outside end of the core was chipped or abraded to a depth of approximately 0.1" over most of the ¾" thick section examined. The inside end of the core had a smooth, paste-rich formed surface. No coatings, deposits, or discoloration was observed on the end surfaces. No major cracks were present. No significant distress was detected. Specific observations are reported below.

<u>Aggregates</u>

The coarse aggregate was well graded quartz and quartzite natural gravel that also contained a few chlorite schist particles. The coarse aggregate particles were rounded to sub-rounded, predominantly hard and dense. Most of these particles had smooth surfaces. Adhesion cracks that extend partially around the aggregate particles were fairly frequent. Paste-aggregate bond was moderately weak. Fresh fractures produced in the laboratory using a geologist's hammer tended to pass around the aggregates. A few quartzite aggregate particles exhibited internal cracking. These cracks were inherent characteristics of the rock and its history before the rock was incorporated into the concrete. No evidence of deleterious reactions involving the coarse aggregates was observed.

The fine aggregate was crushed siliceous sand consisting of angular particles of quartz and quartzite, and smaller amounts of feldspar, mica, iron oxides, and other minerals. No evidence of deleterious reactions involving the fine aggregate was observed. Adhesion cracks that extend partially around the aggregate particles were observed, but were not common features.

Paste

The paste properties were generally good. The paste was light gray, moderately hard, and exhibits a subvitreous to somewhat dull luster. The paste contained abundant partly hydrated Portland cement grains. No supplementary cementitious materials were observed. Calcium hydroxide crystals (portlandite) were abundant, and were moderate in size. Portland cement hydration characteristics appeared to be normal. The extent of cement hydration was moderate. Overall, the paste characteristics were consistent with an estimated water-cement ratio (w/c) of 0.48 to 0.53. In general, the estimated w/c may be higher than the actual w/c if the concrete girder was heat cured.

Paste Carbonation

The paste was surficially carbonated at the formed end and at the outside end of the core.

Air-Void System

The concrete did not appear to be intentionally air entrained. The estimated air content was 2 to 4 percent. This estimate includes entrained air voids having diameters less than or equal to 1 mm, and entrapped air voids having diameters ranging from 1 mm to 10 mm. The smaller air voids were spherical and were uniformly distributed throughout the concrete. The larger air voids were oval to irregularly shaped and occured randomly scattered throughout the concrete.

Joints, Cracks, Microcracks

No joints, cracks or significant microcracks were observed in the examined portion of the core, except for the adhesion cracks that partially surround many of the coarse aggregate particles.

Secondary Deposits

Small amounts of ettringite were detected in a few air voids in the outer portion of the concrete. Ettringite is a secondary mineral deposit, which is evidence of long term exposure to moisture migrating through the concrete.

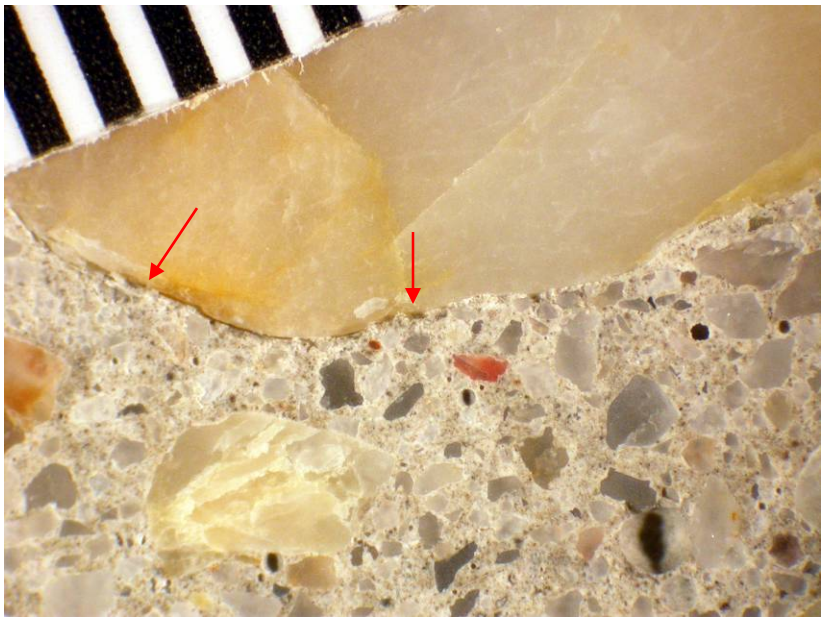

Figure 12. Adhesion crack partially surrounding coarse aggregate particle. Millimeter scale.

Core 138 - Span 162, Girder 3

The inside and outside ends of Core 138 were flat, fairly smooth, paste-rich formed surfaces. The characteristics of the concrete in Core 138 resembled those of Core 17. Differences between the two cores are reported below.

Aggregates

The coarse aggregate, which was predominantly quartzite gravel, contained a few particles of friable orthoquartzite and soft weathered rock. No specific distress was associated with the friable rock. The soft, weathered rock was reactive, but had not caused significant distress. A small amount of alkali-silica gel filled cracks in the peripheral region of the soft particle. These cracks did not extend into the paste.

Paste

Small patches of lighter-colored, porous, and more absorptive paste were common.

Paste Carbonation

The paste was carbonated to a depth of 0.05 to 0.1" at the outside end and to a depth of 0.1" at the interior end.

Air-Void System

The estimated air content was 2 to 3 percent. The concrete contains minor entrapped air voids that were mostly less than 0.08" across, and occasionally 0.1 to 0.3" across.

Secondary Deposits

No secondary deposits were observed.

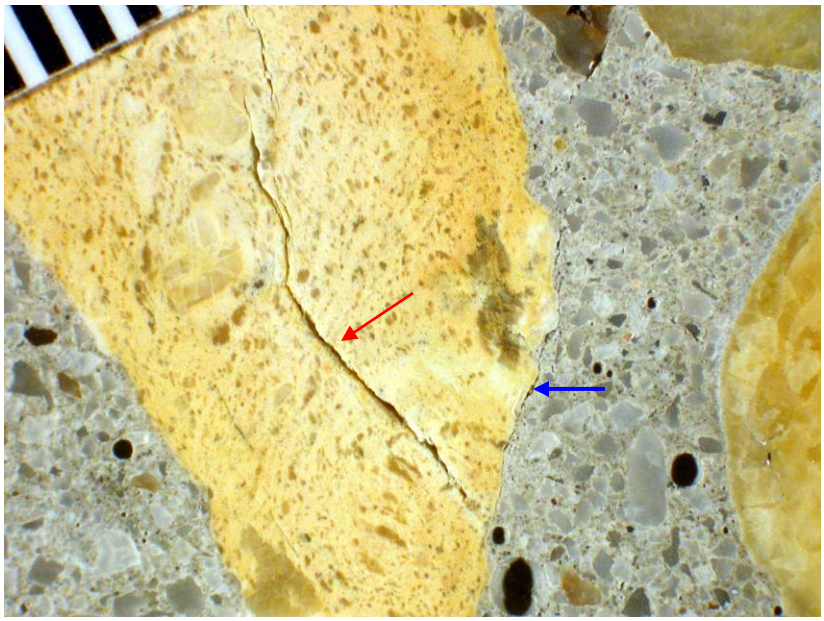

Figure 13. Weathered coarse aggregate particle. Internal cracking (red arrow) unrelated to aggregate reactivity (ASR). Blue arrow shows adhesion crack. Millimeter scale.

Pile Caps

Core 120 - Bent 150 Pile Cap

The concrete contained a fairly well graded calcareous coarse aggregate and a calcareous and siliceous fine aggregate uniformly dispersed in a marginally air-entrained, light to medium gray, Portland cement paste. The estimated air content was 3 to 4 percent. The concrete was well consolidated. The outside end of the core was slightly rough. A thin layer of calcareous deposits partially coats the outer surface. The inside end of the examined portion of the core had a smooth, saw-cut surface. No major cracks were present. However, one microcrack (less than 0.005" wide) extended from the outside surface to a depth of 1.5". On drying, salts crystals formed on the lapped surface of the concrete in the outer 0.7 to 1.5" of the core, indicating that the concrete was reasonably saturated with seawater to these depths. Specific observations are reported below.

Aggregates

The coarse aggregate was a fairly well graded, crushed, marine limestone. The limestone particles were greenish gray, irregularly shaped to sub-rounded, and moderately porous to porous. The maximum size (top size) of the aggregate was 0.8". The limestone consisted of fine to coarse-grained calcite, abundant green glauconite pellets, minor pyrite, various mineral grains (mostly quartz), and casts and fragments of a variety of marine organisms. Shell casts were more abundant in the porous limestone particles. Although frequently empty, these casts sometimes contained dense dark gray cement paste of mortar. Paste-aggregate bond was tight. Fresh fractures produced in the laboratory using a geologist's hammer tended to pass through the aggregates. No evidence of deleterious reactions involving the coarse aggregates was observed.

The fine aggregate was crushed calcareous sand consisting of angular particles of limestone, sub-rounded quartz grains, rounded glauconite pellets, and smaller amounts of other miscellaneous rocks and minerals. No evidence of deleterious reactions involving the fine aggregate was observed.

Paste

The paste properties were generally good. The paste was mottled light, medium, and dark gray. The paste luster and hardness were variable. The luster of the paste was dull to subvitreous locally. The paste hardness was moderately hard to locally soft. Partly hydrated and unhydrated Portland cement grains were moderately abundant. The hydration characteristics of the cement appeared to be normal. The extent of cement hydration was moderately high. No supplementary cementitious materials were observed. Calcium hydroxide crystals (portlandite) were fairly abundant, and were small to moderate in size. Overall, the paste characteristics indicated a variable w/c, estimated to be 0.42 to 0.47 in the dark dense areas of paste and 0.50 to 0.55 in the light gray, softer areas of paste.

Paste Carbonation

The paste was surficially carbonated at the outside end of the core.

Air-Void System

The concrete was possibly marginally air entrained. The estimated air content was 3 to 4 percent. Most of the air voids were small and spherical. These voids were uniformly distributed throughout the concrete, although clusters of voids were observed locally. A small number of larger, irregularly shaped entrapped air voids, occasionally up to 0.3” across, occurred randomly scattered throughout the concrete.

Joints, Cracks, Microcracks

No joints or major cracks were observed. One microcrack extended from the outside surface, intercepted a coarse aggregate particle, and extended along the paste-aggregate boundary to a depth of 1.5”. The body of the concrete contained a few minor microcracks extending between coarse aggregate particles.

Secondary Deposits

Clumps of ettringite needles filled or lined the air voids in the outer portion of the concrete.

Figure 14. On drying, salt crystals appeared on the lapped concrete surface near the outside end of the core.

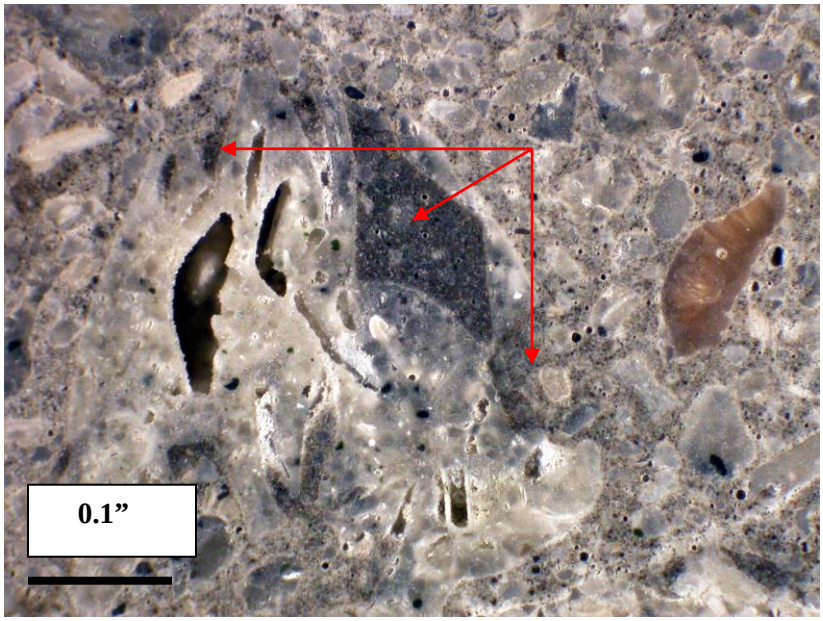

Figure 15. Mottled paste color in the vicinity of a porous limestone aggregate particle. Dark gray paste (red arrows) was hard and dense.

Core 103 - Bent 145 Pile Cap

The outside end of Core 103 was somewhat rough. The concrete was soft, and the paste was discolored and somewhat crumbly to a depth of 0.1" to 0.2". Paste discoloration, but without compromised hardness, extended to a maximum depth of 0.4". The inside end of the portion of the core examined had an uneven surface with an impression of reinforcing steel. The characteristics of this concrete resembled those of Core 120. Differences between the two cores are reported below.

Aggregates

The coarse and fine aggregates were essentially identical to those in Core 120.

Paste

In the body of the concrete the paste color was fairly uniform light gray with occasional dark gray paste/mortar infilling the cavities and voids in the coarse aggregate particles. The paste was pale gray and soft in the outer 0.1 to 0.2". The pale gray layer was underlain by a hard, brownish gray layer about 0.05" thick. This layer was, in turn, underlain by layer having pinkish-orange paste.

Paste Carbonation

The paste was surficially carbonated at the outside end of the core.

Air-Void System

The concrete was air entrained. The estimated air content was 5 to 7 percent. The air voids were small, spherical, and were uniformly distributed throughout the concrete. Clusters of small voids were observed locally. The concrete also contained a small number of irregularly shaped entrapped air voids, typically 0.1" to 0.3" across.

Joints, Cracks, Microcracks

No joints, major cracks, or significant microcracks were observed.

Secondary Deposits

No secondary deposits were observed in the air voids.

Figure16. Paste alteration at the outside end of Core 103. Millimeter scale.

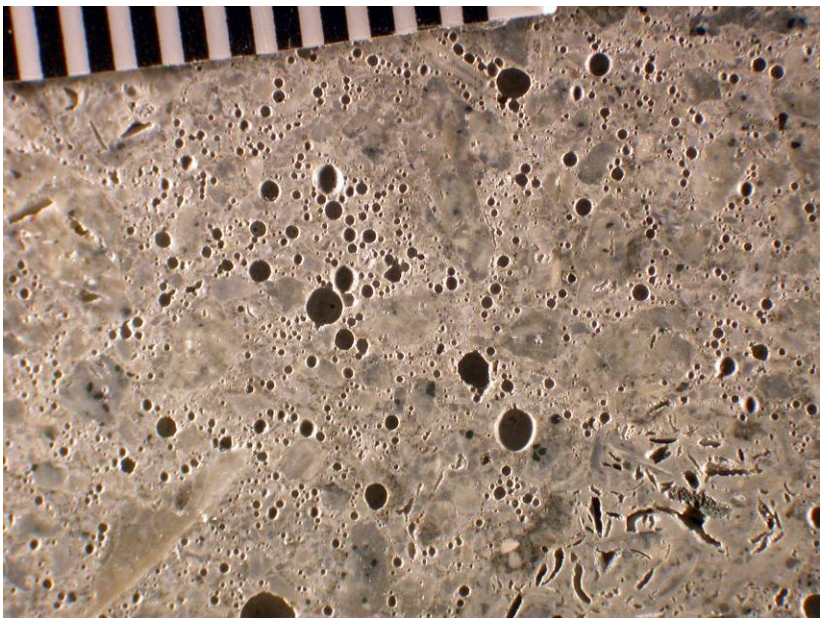

Figure 17. Air entrainment in Core 103.

Bridge Deck

Core 114 - Span 150, Mid-span Deck

The concrete contained a fairly well graded calcareous coarse aggregate and a calcareous and siliceous fine aggregate uniformly dispersed in an air-entrained, mottled gray, Portland cement paste. The estimated air content was 6 to 8 percent. The concrete was well consolidated. The outside end of the core was rough. A thin, discontinuous layer of marine growth and calcareous deposits coated the outer surface. The inside end of the examined portion of the core had an even, paste-rich formed surface. No major cracks were present. Specific observations are reported below.

Aggregates

The coarse aggregate was a fairly well graded, crushed, marine limestone. The top size of the aggregate was 0.7". The limestone particles were typically greenish gray, irregularly shaped to sub-rounded, and were moderately porous to porous. The limestone consisted of fine to coarse-grained calcite, abundant green glauconite pellets, mineral grains, and casts and fragments of a variety of marine organisms. Several particles contained abundant quartz sand grains. A few brown, iron-rich limestone particles were observed. Shell casts were more abundant in the porous limestone particles. Although frequently empty, these casts sometimes contain dense dark gray cement paste of mortar. Paste-aggregate bond was tight. Fresh fractures produced in the laboratory using a geologist's hammer tended to pass through the aggregates. No evidence of deleterious reactions involving the coarse aggregates was observed.

The fine aggregate was crushed calcareous sand consisting of angular particles of limestone, sub-rounded quartz grains, rounded glauconite pellets, and smaller amounts of other miscellaneous rocks and minerals. No evidence of deleterious reactions involving the fine aggregate was observed.

Paste

The paste properties were generally good. The paste was mottled light, medium, and dark gray. The paste luster and hardness were variable. The luster of the paste was dull to subvitreous locally. The paste hardness was moderately hard to locally soft. Partly hydrated and unhydrated Portland cement grains were moderately abundant. The hydration characteristics of the cement appeared to be normal. The extent of cement hydration was variable, but was generally moderately high. No supplementary cementitious materials were observed. Calcium hydroxide crystals (portlandite) were fairly abundant, and were moderate in size. Overall, the paste characteristics indicated a variable w/c, estimated to be 0.42 to 0.47 in the dark dense areas of paste and 0.50 to 0.55 in the light gray, softer areas of paste.

Paste Carbonation

The paste was carbonated to a depth of 0.20 to 0.25" at the outside end of the core. The paste was surficially carbonated at the inside end of the core.

Air-Void System

The concrete was air entrained. The estimated air content was 6 to 8 percent. Most of the air voids were small, spherical, and were uniformly distributed throughout the concrete. Minor clustering of voids were observed locally. The concrete also contained a substantial amount of entrapped air. These voids were 0.05 to 0.4" across, and occurred scattered throughout the concrete.

Joints, Cracks, Microcracks

No joints or major cracks were observed. One microcrack extends from the outside surface to a depth of 0.4". This crack transected a limestone aggregate particle. The body of the concrete did not contain significant microcracks.

Secondary Deposits

Small amounts of ettringite were observed in the air voids in the outer several inches of the concrete.

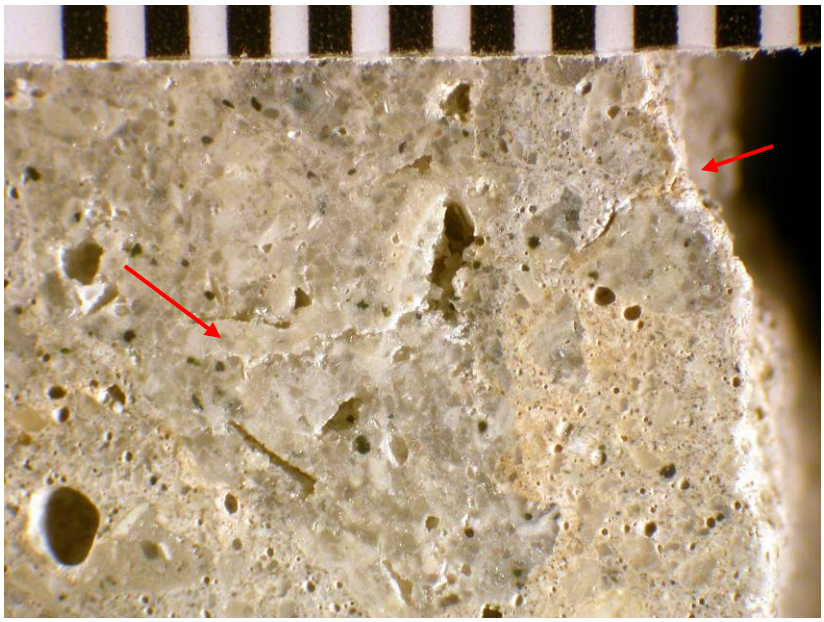

Figure 18. Microcrack extending from the outside surface through a limestone aggregate particle (between red arrows). Millimeter scale.

Core 93 - Span 132, Mid-span Deck

The concrete contained a fairly well graded calcareous coarse aggregate and a calcareous and siliceous fine aggregate uniformly dispersed in an air-entrained, mottled gray, Portland cement paste. The estimated air content was 5 to 7 percent. The concrete was well consolidated. The top surface of the core was slightly uneven and was partially coated with organic growth. The bottom end of the core had an even, paste-rich formed surface that exhibits parallel striations from the concrete form. No major cracks were present. The concrete resembled Core 114. Specific observations are reported below.

Aggregates

The coarse aggregate was a fairly well graded, crushed, marine limestone. The top size of the aggregate was 0.8". The limestone particles were greenish gray, mainly irregularly shaped, and ranged from moderately porous to porous. The limestone consisted of fine to coarse-grained calcite, abundant green glauconite pellets, a variety of mineral grains, and casts and fragments of a variety of marine organisms. A few particles contained abundant quartz and feldspar sand grains. Shell casts were more abundant in the porous limestone particles. Paste-aggregate bond was tight. Fresh fractures produced in the laboratory using a geologist's hammer passed through the aggregates. No evidence of deleterious reactions involving the coarse aggregates was observed.

The fine aggregate was crushed calcareous sand consisting of angular particles of limestone, sub-rounded quartz grains, rounded glauconite pellets, and smaller amounts of other miscellaneous rocks and minerals. No evidence of deleterious reactions involving the fine aggregate was observed.

Paste
The paste properties were fairly uniform and were generally good. The paste was mostly light to medium gray and was moderately hard. Dark gray, dense paste was observed adjacent to some limestone aggregate particles. The paste luster was subvitreous. Partly hydrated and unhydrated Portland cement grains were moderately abundant. The hydration characteristics of the cement appeared to be normal. The extent of cement hydration was moderate. No supplementary cementitious materials were observed. Calcium hydroxide crystals (portlandite) were fairly abundant and were small to moderate in size. Overall, the paste characteristics indicated a moderate w/c, estimated to be 0.45 to 0.50 in the bulk of the paste, and a substantially lower w/c, estimated to be less than 0.40 in areas of dark dense paste.

Paste Carbonation
The paste was carbonated to a depth of 0.30” from the top surface, and 0.25” from the bottom surface of the concrete.

Air-Void System
The concrete was air entrained, and had an estimated air content of 5 to 7 percent. The voids were mostly small, spherical, and were uniformly distributed. The concrete also contained a minor amount of entrapped air scattered throughout the concrete. T hese voids were typically less than 0.1” across.

Joints, Cracks, Microcracks
No joints, major cracks, or significant microcracks were observed.

Secondary Deposits
Small amounts of ettringite were observed in the air voids in the body of the concrete.

Figure 19. Discolored, carbonated paste at the top of Core 93. Millimeter scale.

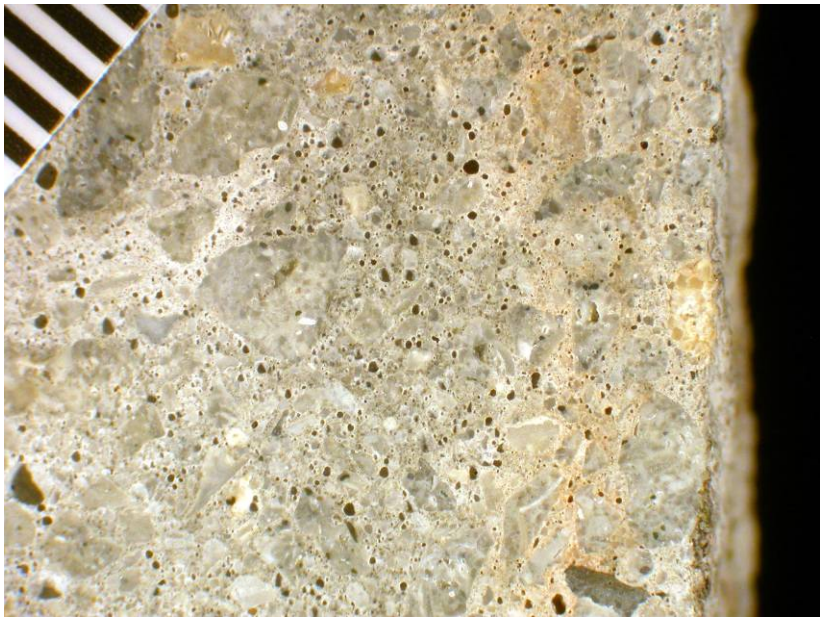

Figure 20. Discolored, carbonated paste at the bottom of Core 93. Millimeter scale.

Core 90 - Span 130, Mid-span Deck

The top surface of the core was slightly rough and uneven, and was partially coated with organic growth. The bottom end of the core had an even paste-rich surface with parallel striations from the concrete form. The concrete was well consolidated. The characteristics of this concrete resembled those of Cores 114 and 93. No major cracks or evidence of significant distress was observed. Differences between the two cores are reported below.

Aggregates

The characteristics of the coarse aggregate were similar to aggregates in Core 93. Some voids in porous limestone aggregate particles were lined with dog-tooth calcite crystals.

The characteristics of the fine aggregate were similar to aggregates in Core 93. The sand contained a small amount of iron-rich particles that had produced localized staining of the paste.

Paste

At the top of the core, the paste was discolored light pinkish beige to a depth of 0.2". The discolored paste was not appreciably softer than the paste in the body of the concrete. Paste in the body of the concrete was mottled light gray, medium gray, and dark gray, suggesting variable w/c ratio.

Paste Carbonation

The paste was carbonated to a depth of 0.20" to 0.25" from the top surface. At the bottom of the core, the paste was surficially carbonated.

Air-Void System

The concrete was air entrained, and had an estimated air content of 4 to 6 percent. Minor clustering of the voids was observed. The entrapped air content was low and these voids were fairly small.

Joints, Cracks, Microcracks

No joints, major cracks, or significant microcracks were observed.

Secondary Deposits

Secondary carbonate deposits occasionally filled or lined small air voids near the bottom surface of the concrete.

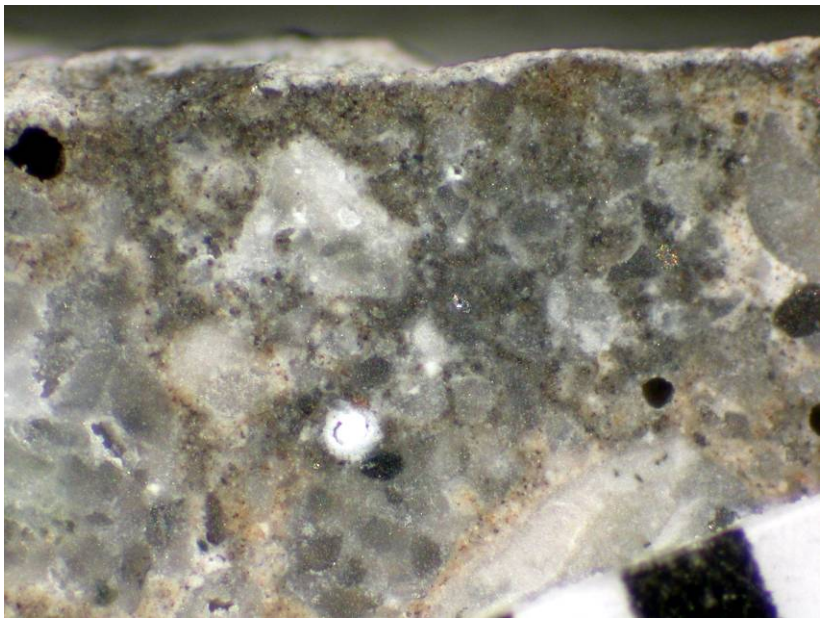

Figure 21. Small voids near the bottom surface of the concrete were lined or filled with secondary carbonate deposits. Millimeter scale.

Core 137 - Span 162, Mid-span Deck

The top surface of the core was slightly uneven and was partially coated with organic growth. The bottom end of the core had an even paste-rich surface that exhibited parallel striations from the concrete form. The concrete was well consolidated. The characteristics of this concrete resembled those of Cores 114, 93, and 90. No major cracks or evidence of significant distress was observed. Differences between the two cores are reported below.

Aggregates

The characteristics of the coarse aggregate were similar to aggregates in Core 93, except that several pinkish limestone aggregate particles near the top and bottom surfaces contained soft deposits within the pores of the aggregate. These aggregates were located within layers of discolored paste (described below). The characteristics of the fine aggregate were similar to aggregates in Core 93.

Paste

At the top of the core, the paste was discolored pinkish beige to a depth of 0.3” to 0.4”. At the bottom of the core, the paste was discolored pinkish beige to a depth of 0.6” to 0.8”. The discolored paste was not appreciably softer than the paste in the body of the concrete. Patches of light gray paste were observed around some of the coarse aggregate particles, possibly indicating that these particles were wet when the concrete was batched.

Paste Carbonation

The paste was carbonated to a depth of 0.20” from the top surface, and 0.40” from the bottom surface of the concrete.

Air-Void System

The concrete was air entrained, and had an estimated air content of 5 to 7 percent. Minor clustering of the voids was observed. The entrapped air content was low and these voids were fairly small.

Joints, Cracks, Microcracks
No joints, major cracks, or significant microcracks were observed.

Secondary Deposits
Minor amounts of ettringite were observed in the air voids in the body of the concrete.

Figure 22. Pores in a coarse aggregate particle near the top surface of Core 137 contain soft, clay-like deposits. Millimeter scale.

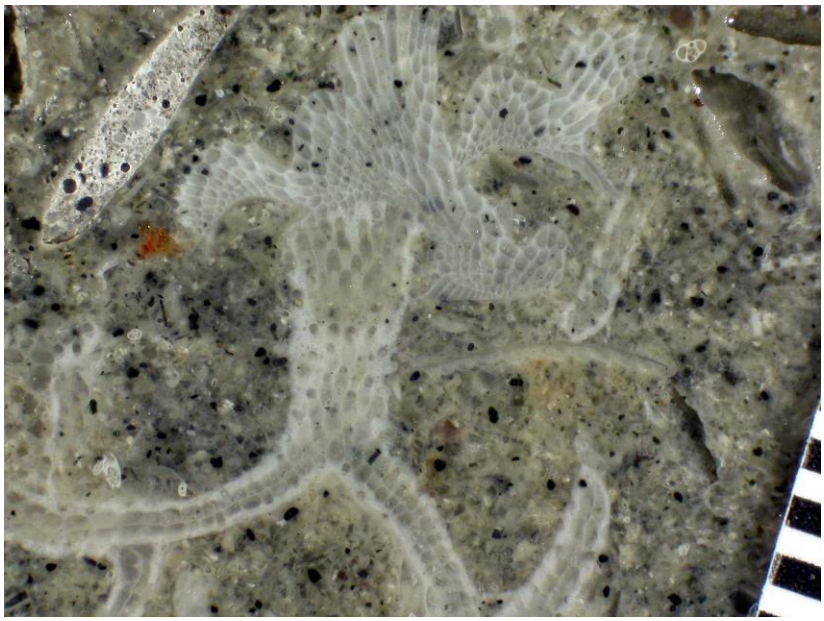

Figure 23. Coralline limestone coarse aggregate particle in Core 137 containing well preserved coral fragments. Millimeter scale.

Columns

Core 104 - Bent 145 Middle Column

The outside surface of the core had a generally even, but locally pitted, paste-rich formed surface. The bottom end of the core had an uneven fracture surface. The concrete was well consolidated. The characteristics of this concrete resembled those of Core 114 and the other concrete cores from the deck. No major cracks or evidence of significant distress were observed. Differences between the cores are reported below.

Aggregates

The characteristics of the coarse aggregate were similar to aggregates in the cores from the deck. Adhesion cracks were observed around portions of several coarse aggregates particles. The characteristics of the fine aggregate were similar to aggregates in the cores from the deck.

Paste

The carbonated paste at the top of the core was discolored light pinkish beige, but was not appreciably softer than the paste in the body of the concrete. Paste in the body of the concrete was generally light gray, with dark gray denser paste adjacent to some of the porous coarse aggregate particles.

Paste Carbonation

The paste was carbonated to a depth of 0.10” from the top surface.

Air-Void System

The concrete was uniformly air entrained, and had an estimated air content of 4 to 6 percent. Entrapped air voids ranging in size from about 0.05" to 0.25" were scattered throughout the concrete, but the entrapped air content was fairly low overall.

Joints, Cracks, Microcracks
No joints, major cracks, or significant microcracks were observed.

Secondary Deposits
Minor amounts of ettringite were observed in air voids in the body of the concrete.

Figure 24. Carbonate crystals line a shell cavity within a limestone coarse aggregate particle.

Figure 25. An adhesion crack (arrows) partially encircles a coarse aggregate particle in Core 104. Millimeter scale.

Core 117 - Bent 150 Middle Column

The outside surface of the core was somewhat rough. The concrete was partially coated with a thin layer of dark gray mortar or grout. Scattered rust-colored specks were embedded in this layer. The bottom end of the core had an uneven fracture surface. The core was fractured and contained a crack when received, and subsequently broke into four segments during preparation for the petrographic examination. One of the fracture surfaces was coated with carbonate deposits, indicating that this fracture occurred before the concrete was cored. The concrete appeared to be well consolidated. The principal characteristics of this concrete resembled those of Core 114, other concrete cores from the deck, and Core 104. Differences between the cores were reported below.

Aggregates

The characteristics of the coarse and the fine aggregates were similar to aggregates in the cores from the deck. Adhesion cracks were observed around portions of several coarse aggregates particles.

Paste

The carbonated paste at the top of the core was discolored pinkish beige to a depth of 0.1” to 0.4”. The discolored paste was not appreciably softer than the paste in the body of the concrete. Paste in the body of the concrete was generally light gray, with scattered patches of dark gray, dense paste adjacent to some of the porous coarse aggregate particles.

Paste Carbonation

The paste was carbonated to a depth of 0.10” to 0.15” from the top surface.

Air-Void System

The concrete was air entrained, with an estimated 3 to 5 percent small, spherical air voids. The air voids were non-uniformly distributed. Portions of the paste contained less than 2 percent air. A small amount of entrapped air was also present.

Joints, Cracks, Microcracks

No joints were apparent. The principal fracture in the core was 1.2" to 2.6" from the outside end of the core. This fracture transected coarse aggregate particles, but did not appear related to any deficiencies in the aggregate particles. Other fracture surfaces appeared to be more recent. The paste exposed by the fractures was unaltered and no secondary deposits were observed. On each side of the fractures, one or two narrow microcracks were observed adjacent to the major fracture. Cracks and microcracks were not observed, except for these features.

Secondary Deposits

Carbonate deposits were observed on the principal diagonal fracture surface. Minor amounts of ettringite were observed in a few air voids in the body of the concrete.

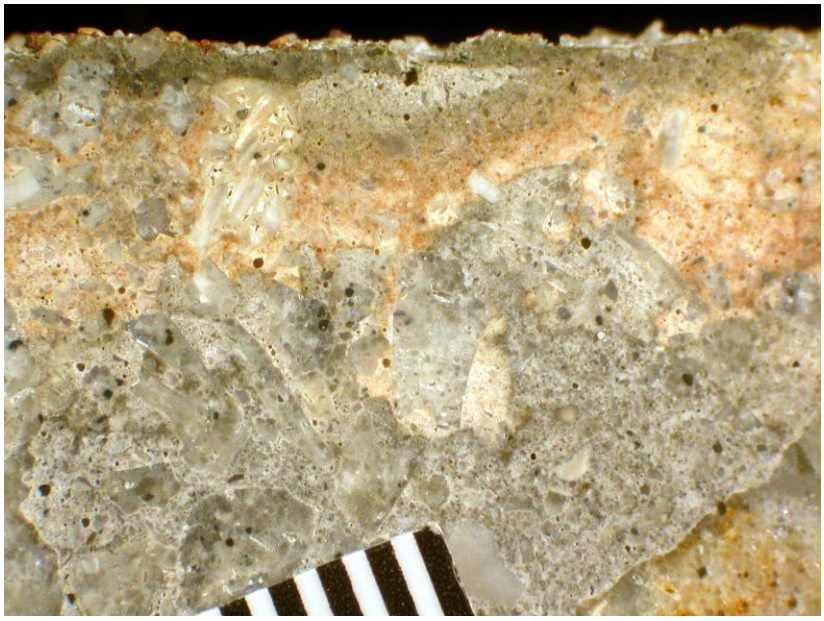

Figure 26. Paste discoloration at the outside end of Core 117. The dark gray layer at the surface was slightly eroded exposing sand grains.

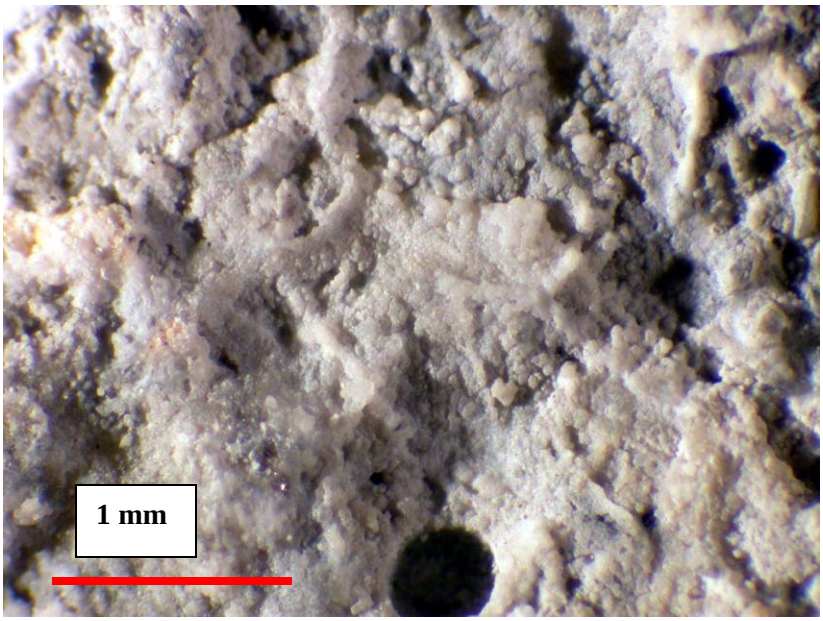

Figure 27. Secondary carbonate deposits coat the outside fracture surface 1.2 to 2.6" from the outside surface. This morphology characterizes open-space filling, and was not considered to be a "cause" of fracturing.

Chloride Analysis

The chloride content was determined for five $^1/_2$" thick slices taken from ten cores. The slices were obtained at depths of $^1/_4$" to $^3/_4$", $1^1/_4$" to $1^3/_4$", $2^1/_4$" to $2^3/_4$", $3^1/_4$" to $3^3/_4$", $4^1/_4$" to $4^3/_4$" then pulverized for acid-soluble chloride analysis according to ASTM C1152, *Standard Test Method for Acid-Soluble Chloride in Mortar and Concrete*. Figure 28 illustrates the slice sampling used.

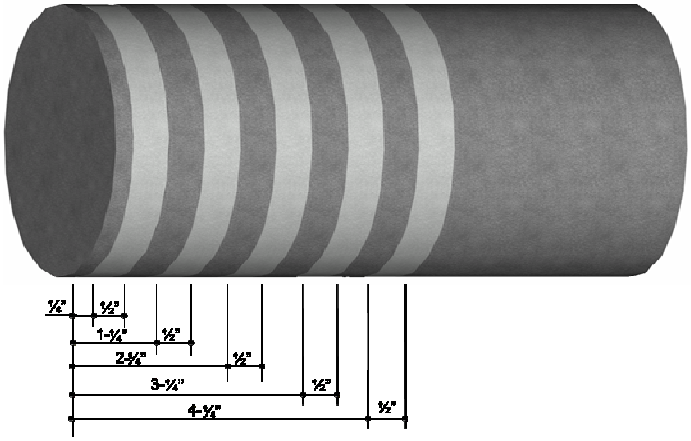

Figure 28. Sampling methodology for chloride tests.

The results are listed in Table 9. The chloride contents for nine of the ten samples are plotted in Figure 29. Note that results from Core 120 are not included in Figure 29 because the magnitude of chloride contents in Core 120 were 2-3 times the levels found in the other cores and adversely affected the scale of the graph. Studies have shown that chloride contents above 0.02 to 0.03 percent by mass of concrete, depending on the cement content, can promote corrosion of embedded steel in non-carbonated concrete. Levels below this threshold can accelerate corrosion in carbonated concrete. Most of the chloride contents were at or above this threshold level and, in the presence of sufficient moisture and oxygen, may promote the corrosion of steel in the concrete.

The following observations were made relative to the chloride content test results:

With the exception of Samples 17, 90, and 114, all the samples tested were found to have chloride levels above the threshold values normally required to promote corrosion actively in embedded steel reinforcement.

Samples 103, 117, and 120 were observed to have chloride contents significantly above those levels found in other samples. Samples 103 and 120 were removed from pile caps and Sample 117 was removed from the west column of Bent 150.

Samples 90, 93, 114, and 137 were removed from the bridge deck. Two of the samples from the bridge deck (93 and 137) were observed to have chloride levels above the threshold values at the depth of the top layer of reinforcement (1 ½”). The other two samples (90 and 114) were observed to have chloride levels slightly below the threshold levels at this depth.

Table 9. Chloride contents[2]

Sample	Location in Bridge	Depth, (in.)	Acid-Soluble Chloride, percent by mass of sample
17	Span 132 Girder G4 Mid-span, mid-height	1/4-3/4 1 1/4- 1 3/4 2 1/4- 2 3/4 3 1/4- 3 3/4 4 1/4- 4 3/4	0.074 0.011 0.005 0.004 0.002
90	Span 130 Deck Mid-span of bridge, 6" from curb	1/4-3/4 1 1/4- 1 3/4 2 1/4- 2 3/4 3 1/4- 3 3/4 4 1/4- 4 3/4	0.025 0.009 0.003 <0.002 0.002
93	Span 132 Deck Mid-span of bridge, 6" from curb	1/4-3/4 1 1/4- 1 3/4 2 1/4- 2 3/4 3 1/4- 3 3/4 4 1/4- 4 3/4	0.046 0.045 0.026 0.015 0.019
103	Bent 145 Pile Cap Southwest corner, vertically from top	1/4-3/4 1 1/4- 1 3/4 2 1/4- 2 3/4 3 1/4- 3 3/4 4 1/4- 4 3/4	0.199 0.193 0.159 0.107 0.066
104	Bent 145 East pier, south face, mid-height	1/4-3/4 1 1/4- 1 3/4 2 1/4- 2 3/4 3 1/4- 3 3/4 4 1/4- 4 3/4	0.075 0.060 0.046 0.024 0.017
114	Span 132 Deck Mid-span of bridge, 6" from curb	1/4-3/4 1 1/4- 1 3/4 2 1/4- 2 3/4 3 1/4- 3 3/4 4 1/4- 4 3/4	0.032 0.017 0.007 <0.002 0.004
117	Bent 150 west pier, west face, mid-height	1/4-3/4 1 1/4- 1 3/4 2 1/4- 2 3/4 3 1/4- 3 3/4 4 1/4- 4 3/4	0.139 0.151 0.082 0.082 0.081
120	Bent 150 Pile Cap South face, east end, horizontal	1/4-3/4 1 1/4- 1 3/4 2 1/4- 2 3/4 3 1/4- 3 3/4 4 1/4- 4 3/4	0.504 0.396 0.270 0.167 0.118
137	Span 162 Deck Mid-span of bridge, 6" from curb	1/4-3/4 1 1/4- 1 3/4 2 1/4- 2 3/4 3 1/4- 3 3/4 4 1/4- 4 3/4	0.048 0.039 0.025 0.011 0.017
138	Span 162 Girder G3 Mid-span, mid-height	1/4-3/4 1 1/4- 1 3/4 2 1/4- 2 3/4 3 1/4- 3 3/4 4 1/4- 4 3/4	0.156 0.046 0.018 0.003 0.010

[2] Data from Core 120 not included in Figure 29 due to scale incompatibility with other data.

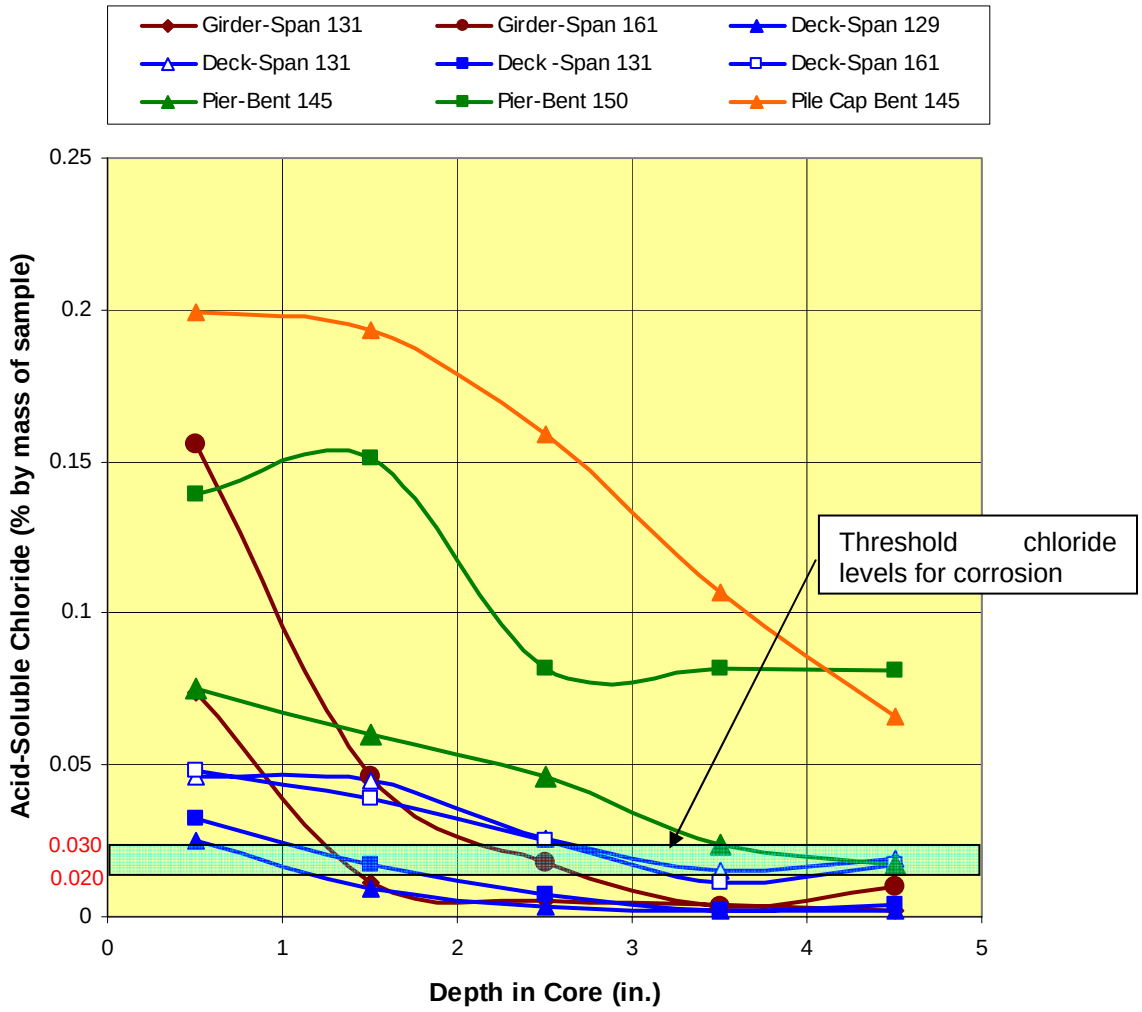

Figure 29. Chloride levels by depth in core. Note data from Core 120 not included in graph due to scale incompatibility.

Concrete Quality

The concrete in the bridge was found to be of high quality. Compressive testing yielded an average strength of 6497 psi for all cores tested, compared to an original design strength of 7,000 psi.

The petrographic examinations also indicate that the concrete was of very good quality. No significant deleterious reactions were observed in any of the core samples. The concrete materials in the pile caps, bent frames, and bridge deck have similar constituent materials and appear to be from the same source. This is consistent with the assumption that concrete for the pile caps, columns, bent caps and bridge deck were supplied from a temporary batch plant near the site. Samples of concrete from the prestressed girders indicated different coarse and fine aggregate materials than those observed in the other concrete

samples as would be expected for girders precast at a permanent plant and shipped to the site. The petrographic examinations also indicated that the depths of carbonation were typically less than 0.25".

UPV measurements confirmed that the quality of the concrete was fairly uniform throughout the structure. Delaminations detected using sounding and visual examinations were confirmed by UPV measurements. No significant internal voids or defects were detected by UPV measurements.

Finally, the chloride content levels in the concrete were evaluated and very high chloride contents were found near the surface (depths less than 1.5") in the bent frames and pile caps. More significantly, the chloride content levels were found to be significantly above the threshold level of 0.02% to 0.03% (by mass of concrete) at depths of up to 4.5". Chloride content levels in the precast girders and the bridge deck were also found to be significantly above the threshold level at depths of 0.5" to 1.0", but at depths of 1.5" the chloride content levels were typically at or below threshold values. The depths of cover for the mild reinforcement and prestressing steel in these superstructure elements were much less than the cover depths observed in the bent components.

Effects of Corrosion Activity

Conventionally, HCP data is interpreted using the Numeric Magnitude Technique specified in Appendix X1 of ASTM C876, *Standard Test Method for Half-Cell Potentials of Uncoated Reinforcing Steel in Concrete*. According to the criteria, "if potentials over an area are more positive than -200 mV vs. CSE, there is a greater than 90 percent probability that no reinforcing steel corrosion is occurring in that area at the time of measurement. If potentials over an area are more negative than -350 mV vs. CSE, there is a greater than 90 percent probability that reinforcing steel corrosion is occurring in that area at the time of measurement. If potentials over an area are in the range of -200 to -350 mV vs. CSE, corrosion activity of the reinforcing steel in that area is uncertain."

These criteria were developed based on laboratory studies simulating bridge decks undergoing chloride-induced corrosion. Since these criteria do not apply to all conditions, particularly where carbonation has occurred, contour maps may be generated using the relative potential magnitudes to estimate corrosion activity. Relative variation of potentials within a test area and the spacing between the contour lines would help indicate areas of active corrosion. If localized areas of more positive potential are surrounded by areas of more negative potential, the area of more positive potential is cathodic or non-corroding, while those of more negative potential are anodic and probably undergoing corrosion. Areas with steep potential gradients would indicate active corrosion. Other variables being equal, maximum corrosion currents will flow between points of high and low potential that are close together and corrosion damage will be the result.

For the prestressed concrete girders, the HCP measurements were typically in the middle zone of -200 to -350mV, providing uncertain indications on the potential for corrosion. Similar values were recorded on the top surface of the bridge deck. The HCP measurements were consistent with the relatively good condition of the concrete in the girders and top surfaces of the bridge deck and the absence of wide-spread delaminations. Note that the localized spalling at the ends of the prestressed girders is likely the result of frequent wetting from water through the joints.

HCP measurements on the pile caps typically yielded potential measurements more negative than -350mV which are indicative of areas of high potential for corrosion activity. These measurements were also consistent with the field observations where delaminations and cracking in the pile caps was wide-spread.

For the columns and bent caps of the high level span bents, the HCP measurements were typically between -200 and -350mV and represented areas where the probability of corrosion was uncertain. These measurements are also consistent with the observed field conditions of moderate cracking and localized areas of spalling.

The process of corrosion deterioration is typically considered to occur in three phases: initiation, propagation, and finally the deterioration itself. The length of the first phase, in which no significant deterioration occurs, is determined by the amount of time required for the steel to become depassivated by chloride ingress or by carbonation. In the propagation phase, active corrosion has begun but insufficient corrosion products have been generated to cause damage. Damage becomes apparent in the third and final phase.

The exposed concrete surfaces throughout most of the bridge structure were minimally carbonated. Field and laboratory tests of carbonation using a phenolphthalein solution detected an affected depth ranging from superficial to about 1/4". For a 40-year old structure, this carbonation depth was less than expected.

Embedded reinforcing bars are normally protected from corrosion because of the high alkalinity (high pH) of the cement paste. Carbonation neutralizes the cement paste whereby the pH is lowered. If the reinforcing bars have a shallow, clear cover and so are located in this carbonated zone, the bars become much more susceptible to corrosion. Corrosion can also be initiated by chlorides from the seaboard environment.

Water leakage through joints in the deck has caused most girders and bent caps beneath the joints to deteriorate. Otherwise, while corrosion in the bridge is ongoing at moderate levels, it is commensurate with corrosion activity in bridge structures constructed in the 1960s and subjected to a severe environmental exposure.

Table 10: Concrete core summary for all cores tested

Bonner Bridge Concrete Core Log															
Legend															
	Denotes high bent cores														
	Denotes approach bent cores														
Core No.	Bent/ Span No.	Member (bent, pile cap, etc.)	Drilling Orientation (H or V)	Core Diam. (in.)	Physical Description	Tests (fc', Cl⁻, etc.)	Original Length (in.)	Trimmed Length (in.)	Depth of Rebar (in.)	Patch Thickness, If Any (in.)	Physical Description	f_c' (psi)	UPV (ft/sec)	Cloride Content Depth - level (in. - % by mass)	Carbonation Depth (in)
1	7	pile cap	H	4	From North face	f_c', UPV	10.75	7.212			porous limestone aggregate	6,920	12,973		
2	12	pile cap	H	4	From South face	f_c', UPV	8	7.309			porous limestone aggregate; uneven exterior face--depressions and 2 small chips	4,990	13,070		
3	13	pile cap	H	4	From North face	f_c', UPV	10.75	7.255			porous limestone aggregate	5,930	12,726		
4	88	pile cap	H	4	From South face	f_c', UPV	10.5	7.3			porous limestone aggregate	6,250	12,361		
5	92-93	girder	H	4	G1, midspan, web midheight	f_c', UPV	7.375				2 formed ends; non-porous aggregate	7,450	13,781		
6	93	pile cap	H	4	From South face	f_c', UPV	10.75	6.193	7		porous limestone aggregate; broken 7 5/8 - 8 ½ in from end; voids on face (large void 5/8" x 1/4") and several small; rebar 0.5" dia	8,550	14,139		
8	102	pile cap	H	4	From South face	f_c', UPV	10.75	7.147	1.25; 2.375		porous limestone aggregate; lines around some aggregates; yellow lines on surface; 1/8" diameter reinforcement	5,600	12,643		
9	103	pile cap	H	4	From North face	f_c', UPV	11.875	7.284			porous limestone aggregate; yellow lines on exterior	6,150	12,543		
10	116	pile cap	H	4	From South face	f_c', UPV	10.375	7.258			porous limestone aggregate; dark material and yellow lines on exterior end	6,290	13,077		
12	117	pile cap	H	4	From North face	f_c', UPV	10.75	7.231			porous limestone aggregate; core says pier cap	5,730	11,488		
13	129-130	girder	H	4	G1, midspan, web midheight, (S-112-113)	f_c', UPV, Carb.	7.5	7.158			2 formed ends; non-porous aggregate	8,310	14,034		top: surficial bottom: surficial
14	129	bent cap		4	From South Elevation, midspan of bent cap	f_c', UPV	10.75				porous limestone aggregate, dark green top surface (partial)	4,420	11,037		
15	129	column		4	From East column, South face, mid-height	f_c', UPV	10.75				porous limestone aggregate	6,580	12,971		
16	129	pile cap		4	From South face, towards west end	f_c', UPV	10.75				porous limestone aggregate	6,320	13,232		
17	131-132	girder	H	4	G1, midspan, web midheight, S-107-108	Cl⁻, Carb.	7.375				2 formed ends; non-porous aggregate			0.25 - 0.75": 0.074 1.25 - 1.75": 0.011 2.25 - 2.75": 0.005 3.25 - 3.75": 0.004 4.25 - 4.75": 0.002	top: surficial bottom: surficial
18	135	bent cap (verify)	H	4	From South face, towards West end; 1.25"-1.5" patch	f_c', UPV	10-10.5	7.204		1.5	porous limestone aggregate, (patch inc. in length)	5,490	13,079		
20	135	top column	H	4	From East column, West face, mid-height; broken	f_c', UPV	8.5	5.624	8	1	porous limestone aggregate, 1.25" dia. rebar, (patch inc. in length - broken off)	7,740	14,555		

Core No.	Bent/ Span No.	Member (bent, pile cap, etc.)	Drilling Orientation (H or V)	Core Diam. (in.)	Physical Description	Tests (fc', Cl⁻, etc.)	Original Length (in.)	Trimmed Length (in.)	Depth of Rebar (in.)	Patch Thickness, If Any (in.)	Physical Description	f_c' (psi)	UPV (ft/sec)	Cloride Content Depth - level (in. - % by mass)	Carbonation Depth (in)
21	135	pile cap (verify)	H	4	From top surface, on North side, centered W-E; 1.5" patch	f_c', UPV	10.25			1.75	porous limestone aggregate, plastic anchor in core, (patch inc. in length)	5,340	12,131		
28	145	bent cap	H	4	From South face, towards East end	f_c', UPV	10.25	7.151			porous limestone aggregate; rust-colored material at inner edge	7,530	13,956		
29	145	pile cap	H	4	From top surface, South-West corner	f_c', UPV	10.5	7.544			porous limestone aggregate	3,830	11,550		
30	145	middle column	H	4	From East column, South face, mid-height	f_c', UPV	10.5	4.698	5.5		porous limestone aggregate; rebar 1.25" dia	7,440	13,641		
31	145	bottom column	H	4	From West column, West face, mid-height	f_c', UPV	10.5				porous limestone aggregate; 3 small pieces of rusty material 7.25 - 8.25" from edge	6,480	13,174		
32	149	middle column	H	4	From East column, West face, ~mid-height	f_c', UPV	10.75				porous limestone aggregate	6,870	12,596		
33	149	pile cap	V	4	From top surface, South-West corner	f_c', UPV	11				porous limestone aggregate	5,720	12,529		
34	149	bottom column	H	4	From West column, West face, 1/3 up	f_c', UPV	10.5				porous limestone aggregate	6,450	13,208		
37	150	bottom column	H	4	From East column, South face; broken	f_c', UPV	11	5.269	6		porous limestone aggregate; broken at rebar (1.25" dia)	7,650	13,895		
39	150	top column	H	4	From West column, East face, mid-height	f_c', UPV	7.5	6.332	7.5		porous limestone aggregate; 0.125" dia rebar	5,780	13,159		
40	150	middle column	H	4	From West column, West face, mid-height	f_c', UPV	4.5 - 6.375	4.392			porous limestone aggregate; rust-like material at inner edge	5,200	13,071		
41	150	pile cap	H	4	From South face, East end	f_c', UPV	10.5	7.578			porous limestone aggregate	6,680	14,125		
53	161	column	H	4	From West column, East face, mid-height	f_c', UPV	10.75				porous limestone aggregate	7,190	13,695		
54	161	bent cap	H	4	From North face, East end	f_c', UPV	8				porous limestone aggregate	6,840	12,684		
55	161	pile cap	H	4	From North face, ~midspan; below water mark	f_c', UPV	11				porous limestone aggregate	7,870	12,792		
56	163	bent cap	H	4	From South face, East end	f_c', UPV	10.5				porous limestone aggregate, large rebar socket on bottom	7,640	12,850		
57	163	column	H	4	From East column, East face, towards top	f_c', UPV	10.5	5.61	6		porous limestone aggregate, 1.25" dia. rebar	8,430	13,914		
58	163	pile cap	H	4	From South face, West end	f_c', UPV	10.5				porous limestone aggregate	5,790	13,158		
63	167	pile cap	H	4	From South face	f_c', UPV	11	7.248			porous limestone aggregate; ridge on exterior face; chipped end; blue X on face	6,400	12,253		
64	175	pile cap	H	4	From North face	f_c', UPV	10.5	4.579	4.75		porous limestone aggregate; 0.5" dia rebar; inner end with large void (0.75 x 0.25")	6,830	13,628		
65	176	pile cap	H	4	From North face	f_c', UPV	10.625	5.835	1.875; 7	4	porous limestone aggregate; patch; 1/8" diameter reinforcement	7,180	13,775		

Core No.	Bent/ Span No.	Member (bent, pile cap, etc.)	Drilling Orientation (H or V)	Core Diam. (in.)	Physical Description	Tests (fc', Cl⁻, etc.)	Original Length (in.)	Trimmed Length (in.)	Depth of Rebar (in.)	Patch Thickness, If Any (in.)	Physical Description	f_c' (psi)	UPV (ft/sec)	Cloride Content Depth - level (in. - % by mass)	Carbonation Depth (in)
66	177	pile cap	H	4	From South face, broke during removal	f_c', UPV	11	4.66	1.75; 2.25; 4.75	4.625 - 5.5	porous limestone aggregate; 0.5" dia rebar at 2.25 and 4.75"; 1/8" dia wire at 1.75"; broken at patch	7,240	12,274		
67	178	pile cap	H	4	From South face	f_c', UPV	11	3.163		6 -7.5	porous limestone aggregate in non-patch: L/D for f'c = 0.92	8,200	14,248		
68	187	pile cap	H	4	From North face	f_c', UPV	6.25 - 7	5.918			porous limestone aggregate; green material and blue X on exterior face	6,310	13,699		
69	190	pile cap	H	4	From South face	f_c', UPV	10.25	7.237			porous limestone aggregate; green material (marine growth) and blue X on end	5,930	12,739		
70	193	pile cap	H	4	From South face, crack thru core	f_c', UPV	11.5	7.246			porous limestone aggregate; badly cracked 0 - 1.75" from end; blue X on end; paste appears discolored	5,890	13,600		
71	201	pile cap	H	4	From South face	f_c', UPV	11.25	7.262			porous limestone aggregate; some dark material and blue X on exterior end	6,080	13,071		
90	129-130	mid-span deck	H	3.5	Approx. 6 in. from curb, at midspan	Cl⁻, Carb.	8.75		3.5		porous limestone aggregate; 0.5" dia rebar			0.25 - 0.75": 0.025 1.25 - 1.75": 0.009 2.25 - 2.75": 0.003 3.25 - 3.75":< 0.002 4.25 - 4.75": 0.002	top: 0.2 - 0.25 bottom: surficial
91	129-130	south deck	H	3.5	Approx. 2 ft from South E.J, and 6 in. from curb	f_c', UPV	8	5.769	7		porous limestone aggregate; 0.5" dia rebar	5,360	13,171		
92	131-132	south deck	H	3.5	Approx. 2 ft from South E.J, and 6 in. from curb	f_c', UPV	7.5	5.454	6		porous limestone aggregate; 0.5" dia rebar	5,310	13,023		
93	131-132	mid-span deck	H	3.5	Approx. 6 in. from curb, at midspan	Cl⁻, Carb.	7.5		5.75		porous limestone aggregate; 0.5" dia rebar; dark material on end			0.25 - 0.75": 0.046 1.25 - 1.75": 0.045 2.25 - 2.75": 0.026 3.25 - 3.75": 0.015 4.25 - 4.75": 0.019	top: 0.3 bottom: 0.25
103	145	pile cap	H	3.5	From top surface, South-West corner	Cl⁻, Carb.	11.75		6.5		porous limestone aggregate; broken at 1.375" dia rebar; no rust around bar socket			0.25 - 0.75": 0.199 1.25 - 1.75": 0.193 2.25 - 2.75": 0.159 3.25 - 3.75": 0.107 4.25 - 4.75": 0.066	0.2
104	145	middle column	H	3.5	From East column, South face, mid-height	Cl⁻, Carb.	7.375				porous limestone aggregate			0.25 - 0.75": 0.075 1.25 - 1.75": 0.060 2.25 - 2.75": 0.046 3.25 - 3.75": 0.024 4.25 - 4.75": 0.017	0.1
113	149-150	girder	H	3.5	From girder #3, at midspan	f_c', UPV, Carb.	8.25	6.471			2 formed ends; non-porous aggregate	6,720	13,977		top: 0.1 bottom: 0.1
114	149-150	mid-span deck	H	3.5	Approx. 6 in. from curb, at midspan	Cl⁻, Carb.	10.5		3		porous limestone aggregate			0.25 - 0.75": 0.032 1.25 - 1.75": 0.017 2.25 - 2.75": 0.007 3.25 - 3.75": <0.002 4.25 - 4.75": 0.004	top: 0.2 - 0.25 bottom: 0.1
115	149-150	south deck	H	3.5	Approx. 2 ft from South E.J, and 6 in. from curb	f_c', UPV	8	3.443	3		porous limestone aggregate; broken 0.5" from end; dark material on end; 0.5" dia rebar	7,470	14,204		

Core No.	Bent/ Span No.	Member (bent, pile cap, etc.)	Drilling Orientation (H or V)	Core Diam. (in.)	Physical Description	Tests (fc', Cl^-, etc.)	Original Length (in.)	Trimmed Length (in.)	Depth of Rebar (in.)	Patch Thickness, If Any (in.)	Physical Description	f_c' (psi)	UPV (ft/sec)	Cloride Content Depth - level (in. - % by mass)	Carbonation Depth (in)
117	150	middle column	H	3.5	From West column, West face, mid-height	Cl^-, Carb.	7				porous limestone aggregate; broken 1.5 - 3.25" from end; crack 3.25" from end			0.25 - 0.75": 0.139 1.25 - 1.75": 0.151 2.25 - 2.75": 0.082 3.25 - 3.75": 0.082 4.25 - 4.75": 0.081	0.1 - 0.15
120	150	pile cap	H	3.5	From South face, East end	Cl^-, Carb.	10.5		6.25		porous limestone aggregate; 0.5" dia rebar			0.25 - 0.75": 0.504 1.25 - 1.75": 0.396 2.25 - 2.75": 0.270 3.25 - 3.75": 0.167 4.25 - 4.75": 0.118	surficial
136	161-162	south deck	H	3.5	Approx. 3 ft from South E.J, and 5 ft from curb	f_c', UPV	7	4.678	5.5		broken at rebar; 0.5" dia rebar; porous limestone aggregate; 1 loose rebar	5,570	13,824		
137	161-162	mid-span deck	H	3.5	Approx. 6 in. from curb, at midspan	Cl^-, Carb.	7.5		5.5		porous limestone aggregate; 0.5" dia rebar; dark material on end			0.25 - 0.75": 0.048 1.25 - 1.75": 0.039 2.25 - 2.75": 0.025 3.25 - 3.75": 0.011 4.25 - 4.75": 0.017	top: 0.2 bottom: 0.4
138	161-162	girder	H	3.5	From girder #2, at midspan	Cl^-, Carb.	7.375				2 formed ends; non-porous aggregate			0.25 - 0.75": 0.156 1.25 - 1.75": 0.046 2.25 - 2.75": 0.018 3.25 - 3.75": 0.003 4.25 - 4.75": 0.010	exterior: 0.05 - 0.1 interior: 0.1
147	175-176	girder	H	3.5		f_c', UPV	7.375					6,200	14,401		

Load Test of Spans 186 and 189

During the 2006 biennial routine inspection of the Bonner Bridge conducted by A&O in March and April 2006, severe deterioration was observed near mid-span of girder G3 in Span 189. A&O reported approximately 11 of the 36 strands were broken or deteriorated at mid-span of the girder. The deteriorated area had been repaired with an epoxy-based repair material but the broken or damaged strands had not been repaired.

As part of the evaluation of the deteriorated condition observed in Span 189, a load test was conducted. The purpose of the load test was to assess the response of girder G3 to a controlled truck loading and evaluate the lateral distribution of the truck loading to adjacent girders. To allow for comparison with a span with no severely deteriorated girders, the load testing was repeated in Span 186. Spans 186 and 189 are located near the south end of the bridge and have fishing catwalks to the east and west.

Summary of Findings

For the dynamic tests, with the test truck centered over Girder G3, the measured strains at the bottom of girder G3 were 51 and 59 microstrain for Spans 186 and 189 respectively. Assuming the concrete in the prestressed girders had a compressive strength of 5,000 psi, these measured strains corresponded to concrete tensile stresses of approximately 205 and 237 psi.

In routine rating of bridge girders, standard AASHTO equations are used to distribute the truck load to the individual girders. The results of the testing described above indicate that these standard equations are overly conservative for this bridge, and that a higher fraction of the truck load is distributed to the adjacent girders. The test also indicates that even for the most severely deteriorated girder, the observed stresses were within allowable limits. For further details on the load test, refer to Appendix E.